

The results obtained from the above methods of analysis of shift and coupling constant data are compiled in Table III.

The limiting shift values given in Table III for the β -D-ribofuranose are similar to those reported for the β -D-lyxofuranose in Table I. This similarity supports the interpretation given for the agreement between the formation constants obtained for calcium and lanthanum binding to these anomers. Additional support for this interpretation can be found in the J_M values for the β -D-ribofuranoside which correspond to the coupling constant expected for the $1C$ conformation.⁶ As in the case of the β -D-lyxofuranose, the δ_M values for the β -D-ribofuranose arise from a combination of complex formation shift and a shift caused by metal-induced changes in the populations of conformers. For the other anomers of D-ribose, the shifts observed upon complexation with metal ions must arise solely from complex formation shifts, since no metal-induced changes in conformation are expected.

As already indicated, the results of the plots of observed shifts against observed coupling constants (cf. Figure 7) can be used to check the results obtained from the plots of $\delta/[M]$ against δ . Comparisons of the δ_M values obtained from these two methods are in good agreement, showing that all the methods employed are at least internally consistent. In addition, the values for J_0 reported here are in good agreement with those measured from the spectra of D-ribose in the absence of any metal ions. These two observations serve to justify the use of eq 20 and 21 to analyze the shift and coupling constant data obtained from treatment of D-ribose with metal ions.

Conclusions

The methodology outlined here can be applied to analyze

the interactions of simple carbohydrates with metal ions. From the results of these procedures it is clear that 1:1 metal-sugar complexes are formed in aqueous solution. The present results bear out previous suggestions that the binding of metal ions to pyranoses occurs with the pyranose ring in a conformation which contains an ax-eq-ax arrangement of three consecutive hydroxyl groups.

Acknowledgment. This work was supported by a grant from the United States-Israel Binational Science Foundation.

References and Notes

- (1) Address correspondence to this author.
- (2) For a review see: J. A. Rendleman, Jr., *Adv. Carbohydr. Res.*, **21**, 209 (1966).
- (3) (a) S. J. Angyal and K. D. Davies, *Chem. Commun.*, 500 (1971); (b) S. J. Angyal, D. Greeves, and V. A. Pickles, *Carbohydr. Res.*, **35**, 165 (1974); (c) S. J. Angyal, *Tetrahedron*, **30**, 1695 (1974).
- (4) S. J. Angyal, *Aust. J. Chem.*, **25**, 1957 (1972).
- (5) S. J. Angyal, *Pure Appl. Chem.*, **35**, 131 (1973).
- (6) For a recent review of NMR in carbohydrate see: G. Kotowycz and R. U. Lemieux, *Chem. Rev.*, **73**, 669 (1973).
- (7) G. Scatchard, *Ann. N.Y. Acad. Sci.*, **51**, 660 (1949).
- (8) D. A. Deranleau, *J. Am. Chem. Soc.*, **91**, 4044 (1969).
- (9) D. A. Deranleau, *J. Am. Chem. Soc.*, **91**, 4050 (1969).
- (10) For a review of the methods of measurement of binding constants using NMR measurements see: R. C. Foster and C. A. Fyfe, *Prog. Nucl. Magn. Reson. Spectrosc.*, **4**, 1 (1969).
- (11) A. I. Vogel, "A Textbook of Quantitative Inorganic Analysis", Wiley, New York, N.Y., 1961, pp 259-260.
- (12) M. M. Woyski and R. E. Harris, *Treatise Anal. Chem.*, **8**, 57 (1963).
- (13) (a) R. U. Lemieux and J. D. Stevens, *Can. J. Chem.*, **44**, 249 (1966). (b) Conformers $1C$ and $1C'$ correspond respectively to 1C_4 and 4C_1 ; according to the new rules: *J. Chem. Soc., Chem. Commun.*, 505 (1973).
- (14) S. J. Angyal, *Angew. Chem., Int. Ed. Engl.*, **8**, 157 (1969).

Poly(γ -benzyl L-glutamate) Helix-Coil Transition. Pretransition Phenomena in the Liquid Crystal Phase¹

Russell W. Duke,^{2a} Donald B. Du Pré,^{2a} William A. Hines,^{2b} and Edward T. Samulski*^{2b}

Contribution from the Department of Chemistry, University of Louisville, Louisville, Kentucky 40208, and the Departments of Physics and Chemistry and Institute of Materials Science, University of Connecticut, Storrs, Connecticut 06268. Received September 4, 1975

Abstract: Measurements of the macroscopic properties of synthetic polypeptide liquid crystals indicate that the helix-coil pretransition behavior parallels that reported in dilute solution studies. As varying amounts ($\leq 10\%$ by volume) of TFA were added to PBLG in dioxane (24 mg/cm³ dioxane), observations were made on the pitch in zero magnetic field; in orientated nematic structures of the same liquid crystals, measurements of the diamagnetic susceptibility anisotropy, $\Delta\chi$, and the reorientation rate in a magnetic field were made. The results obtained indicate that the asymmetric part of the intermolecular potential increases across the pretransition range while the twist elastic constant K_{22} remains unchanged. Even small amounts of TFA ($\sim 1\%$ by volume) are sufficient to induce a sharp increase in the fluidity, reminiscent of the behavior of dilute, isotropic solutions of PBLG (i.e., breakdown of an aggregated network). In addition, this work demonstrates that extracting microscopic polypeptide side chain structural information from $\Delta\chi$ measurements is feasible. Specifically, the average orientation of the PBLG side chain as well as its mobility can be monitored as TFA is added to the liquid crystal. The sum of evidence supports the idea that, in the pretransition region, the helix remains rodlike while there is an increased mobility of the side chain as TFA is added.

I. Introduction

The helix-coil transition continues to stimulate considerable interest among both theorists and experimentalists. Over the last two decades, the former have produced numerous new or refined mathematical models which exhibit order-disorder

phase transitions with provisions for fitting the abruptness of the transition "cooperativity" to experimental observations of the helix-coil transition.^{3a} And, as new physical parameters become experimentally accessible, the measurement and usefulness of such parameters are frequently demonstrated via

this dramatic *intramacromolecular* transition. However, the sustained attention devoted to the helix-coil transition by researchers from various disciplines has not yet yielded a concise picture of its molecular details. Controversy centers in particular on the mechanism of the acid-induced helix-coil transition in binary solvent systems.

For the most part, dilute solutions of synthetic polypeptides (usually, poly(γ -benzyl L-glutamate) (PBLG)) have been employed for model investigations of the helix-coil transition. A variety of experimental techniques have shown that in mixed solvent systems containing between 10 and 30% trifluoroacetic acid (TFA) by volume (depending on the solvent and molecular weight of the polypeptide), PBLG will change from a rigid, rodlike, α -helical polymer to a flexible, random-coil polymer.^{3b} In addition, the literature contains many reports of subtle, gradual changes in experimental parameters used to monitor the state of the polypeptide across the range 1–10% TFA, prior to the precipitous change in the parameter at the helix-coil transition itself (see references cited in ref 3c and 4). Various theories have surfaced to account for pretransition behavior caused by halogenated acids in the low acid concentration range: the disruption of aggregated PBLG helices,⁵ the gradual “unfreezing” of the PBLG side chains on the periphery of the macromolecule with increasing TFA,⁶ the “melting” of low molecular weight helices to random coils in polydisperse PBLG samples.⁷ We take a different approach to pretransition phenomena, i.e., investigation of polypeptides in a highly aggregated liquid crystalline state. We select this approach because liquid crystals are ideally suited for quantitative experimental measurements of novel macroscopic properties that are related to changes in the polypeptide molecular conformation.

The large axial ratio of the high molecular weight helical PBLG rods underlies an essentially entropically driven phase transition from an isotropic solution to a lyotropic liquid crystal in concentrated PBLG solutions.⁸ The inherent asymmetry of the α helix and resulting asymmetric *intermacromolecular* potential produces a cholesteric structure in the PBLG liquid crystal closely related to that formed in thermotropic liquid crystals. This cholesteric *supramolecular* structure is exhibited as a pattern of parallel, equispaced retardation lines when the liquid crystalline solution is viewed normal to the cholesteric twist axis.⁹ The viscoelastic properties of the liquid crystal are characterized by a set of elastic moduli, K_{ij} , and viscosity coefficients, γ_i . These parameters are fundamental in the establishment of the liquid crystal, and, together with its diamagnetic (dielectric) anisotropy, describe the response of the liquid crystal to external perturbations such as magnetic (electric) fields. In this paper, we examine the effect of TFA on the liquid crystalline phase of PBLG and relate observed changes in its macroscopic properties to previously reported phenomena in dilute solution studies of the helix-coil transition. Measurement of the diamagnetic anisotropy of the liquid crystal affords a method for quantitatively monitoring changes in the polypeptide side chain secondary structure prior to the TFA-induced transition.

II. Experimental Section

Several years ago it was discovered that the cholesteric structure of PBLG liquid crystals could be transformed into an oriented nematic structure, given a sufficiently strong magnetic field.¹⁰ The field-induced structural transition is slow, requiring several hours in some cases. In the resulting arrangement, the rodlike helices are aligned parallel to the field. The slowness of response of this polymeric liquid crystal to external stimuli, in contrast to thermotropic liquid crystals, facilitates a number of physical measurements.

All of the magnetic measurements were made with a modified vibrating sample magnetometer, Model 155, Princeton Applied Research Corp. (See ref 11 for experimental details.) Magnetic fields up to 20 kOe and temperatures from room temperature to 70 °C were

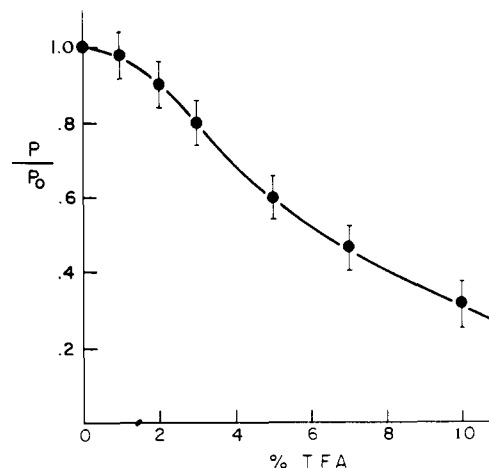


Figure 1. The pitch of the cholesteric structure, P , normalized by the value for 0% TFA, P_0 , as a function of % TFA (vol) in PBLG-dioxane:TFA liquid crystals (24 mg polymer/cm³ dioxane).

available with the related accessories. Direct optical observations of the spacing between retardation lines in the cholesteric liquid crystal were possible with a 70X polarizing microscope.

The synthetic polypeptides were supplied by Pilot Chemical Co. (New England Nuclear). Polypeptide solutions were matured for at least 1 week to ensure complete solubilization of the polymer and homogeneity of the liquid crystal. In most cases, the development of the pattern of retardation lines occurred within a few days.

Unless otherwise indicated, all liquid crystal samples used for the experimental measurements consisted of solutions of PBLG (mol wt = 300 000) in dioxane (24 mg polymer/cm³ dioxane) to which varying amounts of TFA were added.

III. Results

A. Cholesteric Pitch. The *supramolecular* structure exhibited by PBLG liquid crystals, the cholesteric structure, is characterized by the pitch P_0 of the helicoidal arrangement of α -helical macromolecules about an axis of torsion. (The subscript “0” indicates an absence of external fields and/or acid which perturbs the equilibrium value of the pitch.) In those macroscopic regions of the bulk sample which are viewed along a direction normal to the axis of torsion, the cholesteric texture is manifested as a series of parallel, equispaced, retardation lines of spacing $P_0/2$. In the liquid crystalline PBLG solution, P_0 is of the order of 1–100 μm , and varies with temperature and with PBLG concentration, c , in an inverse manner ($P_0 \propto 1/c^2$).⁸

Utilizing the polarizing microscope to observe the retardation lines, the variation of the pitch for the PBLG-dioxane:TFA liquid crystal in zero magnetic field was determined as a function of TFA concentration (vol %). In Figure 1, the data have been normalized to the value of the pitch in the absence of TFA, $P_0 = 47 \mu\text{m}$. The effect of TFA is minimal below 2%. After this initial insensitivity, the pitch decreases more rapidly with TFA concentration in the remainder of the pretransition range (1–10% TFA; the helix-coil transition, determined by changes in the chemical shift of the ^1H proton,¹² occurs at $\sim 25\%$ TFA (vol)).

B. Twist Elastic Constant and Critical Magnetic Field. Application of a sufficiently strong magnetic field will untwist the cholesteric structure to form an aligned nematic structure.¹⁰ Meyer¹³ and de Gennes^{14,15} have derived independently a theoretical relationship between the pitch of a cholesteric structure, P , and the applied magnetic field, H . They predict an increase in the pitch as the applied field is increased with a logarithmic divergence of P when the field strength approaches a critical value. This behavior has been verified for lyotropic cholesteric polypeptide liquid crystals by Duke and

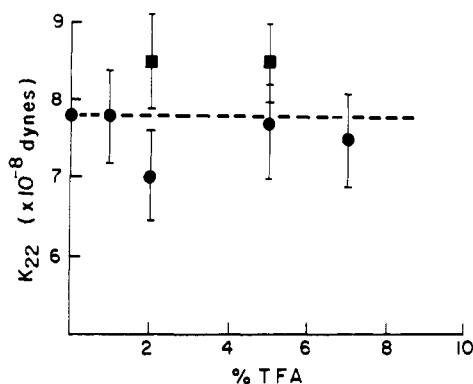


Figure 2. The twist elastic constant, K_{22} , as a function of % TFA (vol) in PBLG-dioxane:TFA liquid crystals; (●) PBLG mol wt = 300 000; (■) PBLG mol wt = 310 000.

Du Pré.¹⁶ In addition, theory relates the critical field, H_c , the initial pitch, P_0 , the twist elastic constant, K_{22} , and the diamagnetic anisotropy, $\Delta\chi$, as follows

$$H_c = \pi^2(K_{22}/\Delta\chi)^{1/2}/2P_0 \quad (1)$$

The variation of H_c for increasing TFA concentration has been previously determined.¹⁷ With the value of P_0 (section A), we calculate $(K_{22}/\Delta\chi)$ from eq 1. An independent magnetometer measurement of $\Delta\chi$ is required (see section C) in order to determine the behavior of K_{22} when the TFA concentration is changed. Figure 2 shows the variation of K_{22} as TFA is added to the PBLG-dioxane:TFA liquid crystal. Within experimental error, K_{22} appears insensitive to TFA concentration in the pretransition range.

C. Diamagnetic Anisotropy. During the field-induced cholesteric-nematic transition ($H > H_c$), a time-dependent anisotropy in the observed magnetic moment, $\Delta\mu(t)$, develops in the liquid crystal.¹¹ The untwisting and alignment process is easily explained by the fact that, for the α -helical rodlike polypeptide molecules, the susceptibility per peptide residue along the longitudinal axis of the rod, σ_{\parallel} , is diamagnetically smaller than the average transverse susceptibility per residue, σ_{\perp} (axially symmetric rods). Hence, the system will take on a configuration of minimum energy in an applied magnetic field when the rods align parallel to the field. The resulting diamagnetic anisotropy per mole of peptide residues of a macroscopically aligned nematic, $\Delta\chi$, will be given by

$$\Delta\chi = (\chi_{\parallel} - \chi_{\perp}) = N_A(\sigma_{\parallel} - \sigma_{\perp})S \quad (2)$$

where N_A is Avogadro's number and $S = \langle \frac{1}{2}(3 \cos^2 \theta - 1) \rangle$ is the order parameter describing the angular deviation of the longitudinal axes of the rods from the nematic director caused by thermal motion.¹⁸ By observing $\Delta\mu(t)$ as a function of time, we can obtain a value for $\Delta\chi$ by writing $\Delta\chi = \Delta\mu(\infty)/nH$ where $\Delta\mu(\infty)$ is the asymptotic value of $\Delta\mu(t)$ for large t , H is the applied magnetic field, and n is the number of moles of polypeptide residues. (In order to calculate values for the twist elastic constant K_{22} and the rotational viscosity coefficient γ_1 , sections B and D, respectively, it is necessary to express $\Delta\chi$ in units of emu per cm³ of liquid crystal.¹⁹)

The measured value of $\Delta\chi$ in the PBLG-dioxane:TFA liquid crystal reflects the anisotropy of the polypeptide only. This is so because the solvent molecules are only slightly oriented (solvent order parameters in these liquid crystals determined with NMR, even in the case of specific solvent-polymer binding, are of the order of 0.001²⁰). Hence, changes in $\Delta\chi$ for PBLG liquid crystals having binary solvent systems which occur on changing the relative amounts of the two solvents reflect changes in the susceptibility of the macromolecule ($\sigma_{\parallel} - \sigma_{\perp}$) and/or changes in S .

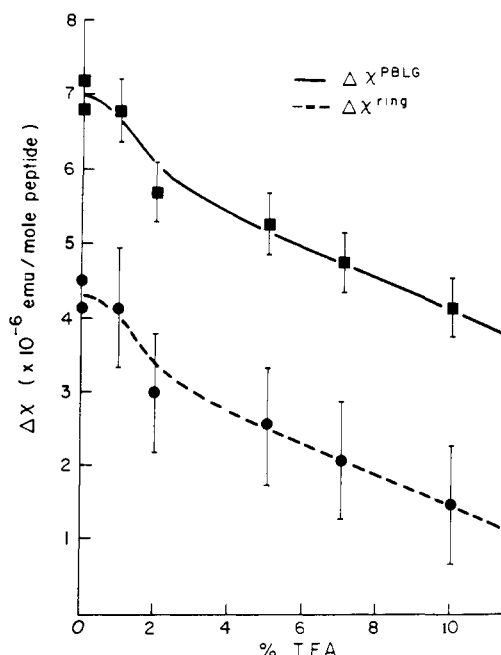


Figure 3. The anisotropy of the diamagnetic susceptibility of PBLG-dioxane:TFA liquid crystals as a function of % TFA (vol) (■, —). The anisotropy of the diamagnetic susceptibility of the benzyl fragment of the PBLG side chain in PBLG-dioxane:TFA liquid crystals as a function of % TFA (vol) calculated from eq 4 with $\Delta\chi^{\text{PGA}} = 2.58 \times 10^{-6}$ emu/mol (●, - - -).

In Figure 3 (solid line), the observed diamagnetic anisotropy of the PBLG-dioxane:TFA liquid crystal is shown as the TFA fraction is increased. For expediency, TFA was added to a PBLG-dioxane liquid crystal in subsequent steps, i.e., the fraction of polymer in the liquid crystal decreases across the range 1–10% TFA. However, the observed decrease in $\Delta\chi$ exceeds considerably that anticipated from mere dilution of polypeptide. High resolution NMR studies show that PBLG ester hydrolysis by TFA is very small on the time scale of these experiments; the decrease in $\Delta\chi$ cannot be attributed to chemical degradation of the side chain.²¹

D. Rotational Viscosity Coefficient. Once the cholesteric structure has been completely untwisted and the rods aligned in a magnetic field $H > H_c$, the resulting nematic director can be quickly rotated with the magnetometer to any desired orientation in the field ($\phi = \phi_0$) and $\Delta\mu(t)$ can be observed as a function of the time during which the nematic director realigns with the field ($\phi = 0$). The realignment is driven by the magnetic torque $T_{\text{mag}} = -\frac{1}{2}(\Delta\chi)H^2 \sin(2\phi)$ and opposed by a viscous torque $T_{\text{vis}} = -\gamma_1(d\phi/dt)$ which defines the rotational viscosity coefficient γ_1 . In ref 11, we describe the mathematical details of relating $\phi(t)$ to $\Delta\mu(t)$ and the subsequent calculation of $\gamma_1 = \tau(\Delta\chi)H^2$ where τ is the characteristic "time constant" for reorientation.

Figure 4 presents the change in $\Delta\mu(t)$ as a function of time occurring in the PBLG-dioxane:TFA liquid crystals with 0, 1, and 2% TFA after setting $\phi = \phi_0 = 90^\circ$ at $t = 0$ ($H = 18$ kOe); the values of γ_1 are 2.7×10^3 , 8.4×10^2 , and 6.4×10^2 P, respectively. It can be seen that the rate of reorientation increases dramatically with the addition of small amounts of TFA. The calculated value of γ_1 decreases by a factor of 4 with addition of $\sim 1\%$ TFA. Reorientation rates for higher TFA concentrations ($>2\%$) are too fast for accurate determination with the magnetometer. NMR studies of this process yield plots of the temporal development of solvent dipolar splittings and suggest that after the abrupt increase in the reorientation rate at 1%, γ_1 does not decrease significantly at higher TFA concentrations.²² The determination of γ_1 using solvent NMR spectra has recently been reported for PBLG liquid crystals.²³

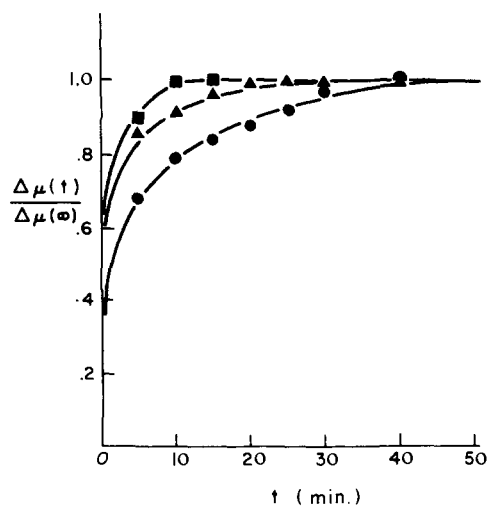


Figure 4. The change in the anisotropy of magnetic moment as a function of time for oriented, nematic PBLG-dioxane:TFA liquid crystals; at $t = 0$, the nematic director is aligned perpendicular to the magnetic field: (●) 0% TFA, (▲) 1% TFA, (■) 2% TFA.

IV. Discussion

A. Macroscopic Properties. The cholesteric structure which forms spontaneously in this class of liquid crystals is an unusual macroscopic manifestation of certain aspects of the conformation of the polypeptide molecule. The sign of the form optical rotation²⁴ is a measure of the sense of the cholesteric twist. It is positive for cholesteric structures with a right-handed twist and negative for structures with a left-handed twist. The sense of the cholesteric twist is dependent on the chirality of the constituent molecules *and* the solvent used in the liquid crystal. For example, in liquid crystals with dioxane as a solvent, the right-handed α -helix PBLG generates a cholesteric structure with positive form optical rotation and the left-handed α -helix PBDG (a homopolypeptide with D-amino acids) generates a cholesteric structure with negative form optical rotation. Independent of solvent, liquid crystals containing a racemic mixture of PBLG and PBDG exhibit no form optical rotation, i.e., they form the untwisted nematic structure.

Robinson⁸ noted an unusual behavior of the pitch and sense of the cholesteric structure when PBLG liquid crystals were prepared in various neat and mixed solvents. As noted above, PBLG-dioxane liquid crystals have positive form optical rotation; however, PBLG- CH_2Cl_2 liquid crystals have negative form optical rotation. In both solvents, the PBLG α helix is right-handed.^{3b,25} The situation is exactly reversed for PBDG. Figure 5 shows the change in the form optical rotation ($2/P_0$) for liquid crystals prepared in binary solvent mixtures. P_0 increases as the fraction of polar solvent in dioxane: CH_2Cl_2 or dioxane:nitrobenzene mixtures is increased. At a critical ratio of solvents, $P_0 \rightarrow \infty$, the cholesteric structure is compensated (becomes an untwisted nematic structure) and the form optical rotation changes sign.

Goossens has presented a general theory relating the origin of cholesteric twist to molecular chirality.²⁶ He derives an angular dependent intermolecular potential for planar molecules whose long axes lie in adjacent "twist planes" separated by a distance r_{ab} :

$$-V_{ab} = \left(\frac{A}{r_{ab}^4} \cos 2\theta_{ab} + \frac{B}{r_{ab}^5} \sin 2\theta_{ab} \right) \quad (3)$$

The planes are perpendicular to the cholesteric axis; θ_{ab} is the angle between the directions of the long axis alignment in respective planes a and b . The coefficient of the symmetric part of this potential, A , is related to the anisotropy of the molecular polarizability. The cholesteric twist occurs because of the

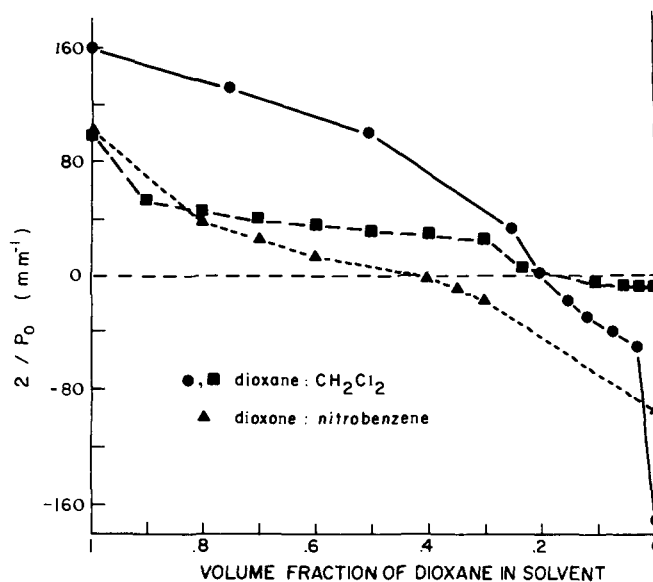


Figure 5. The form optical rotation, $2/P_0$, for cholesteric textures in PBLG liquid crystals with mixed solvent systems: (●) data for the binary solvent dioxane: CH_2Cl_2 (unspecified PBLG concentration);⁸ (■) dioxane: CH_2Cl_2 (PBLG concentration, 20 mg polymer/ cm^3 solvent); (▲) dioxane:nitrobenzene (PBLG concentration, 20 mg polymer/ cm^3 solvent).

asymmetric part of the potential; B is related to the dispersion energy determined by electric dipole-electric quadrupole interactions. The magnitude of the twist, θ_{ab} , is proportional to the ratio $B/r_{ab}A$.²⁶

This theoretical relation between molecular chirality and cholesteric twist, admittedly derived for thermotropic liquid crystals without cylindrical symmetry, nevertheless prompts us to speculate that some type of polypeptide conformational change resulting in a change of the *apparent* chirality of PBLG is responsible for the intriguing behavior of P_0 shown in Figure 5 (see ref 44).

In the past, the concept of a regular side chain secondary structure on the exterior of PBLG has been often discussed.^{3c,4} (In this context, side chain secondary structure refers to a dynamic, regular arrangement of the PBLG side chains resulting from a minimization of steric constraints and an enhancement of electrostatic interaction between neighboring side chain chromophores.) In fact, the usually low electric dipole moment of PBLG peptide residues has been attributed to a specific antiparallel orientation of the dipole of the ester in the side chain relative to that of the amide in the backbone.²⁷

Earlier, Samulski suggested that changes in the *apparent* chirality of the polypeptide could be accomplished through alterations of the side chain secondary structure while leaving the handedness of the helical backbone unperturbed.²⁸ The magnitude of the angular displacements on the molecular scale of one PBLG rod relative to its nearest neighbor in dioxane and CH_2Cl_2 is very small (θ_{ab} is only minutes of arc).⁸ This suggests that the overall differences in the chiral appearance between the van der Waals surface of PBLG in dioxane and its "mirror image" in CH_2Cl_2 is rather small. It seems plausible that comparatively inert solvents such as CH_2Cl_2 and dioxane with variable polarity, dielectric constant, etc., could effect nonbonded interactions between side chain chromophores which stabilize or destabilize specific side chain secondary structures, i.e., the chiral sense of the PBLG exterior could change with solvent and result in a change in sign of B (eq 3) and P_0 (Figure 5).

The tightening of the cholesteric twist observed on increasing TFA concentrations (Figure 1) indicates that the magnitude of the asymmetric part of the intermolecular potential increases

across the pretransition range. This observation is compatible with a superficial conformational change of the PBLG molecule caused by specific TFA interactions with the side chain. In terms of Goossens' theory, the resulting change in the "appearance" of the PBLG rod would have to amplify asymmetric electrostatic interactions between rods (increase θ_{ab}) and thereby decrease P_0 . Below in part B we show that TFA disrupts PBLG side chain secondary structure. In order to remain consistent, we deduce that adding TFA increases θ_{ab} by eliminating a side chain conformation which attenuates $B/r_{ab}A$. In other words, this side chain conformation, when intact, partly cancels the contribution to the asymmetric part of V_{ab} made by the helical array of permanent electric dipoles on the polypeptide backbone.

Physically, the twist elastic constant, K_{22} , describes the force necessary to induce a twist deformation in the cholesteric structure, either mechanically, through an external field, or by natural thermal excitations. The twist elastic constant is dependent on short range and long range order in the liquid crystal. In principle, K_{22} can be related to the intermolecular potential through the appropriate derivatives of a partition function. Although TFA changes the equilibrium angular orientation of one PBLG molecule relative to its neighbor (θ_{ab}), K_{22} does not change in the pretransition range (Figure 2). P_0 is related to the ratio of the coefficients in eq 3 and K_{22} , presumably, is a function of V_{ab} . However, since $B \ll A$, a sizable change in P_0 is not necessarily accompanied by a comparable change in K_{22} . Polypeptide concentration, molecular weight, and solvent in the liquid crystal do influence K_{22} .^{11,17}

The abrupt change in the rotational viscosity coefficient, γ_1 , with the addition of small amounts of TFA to the liquid crystal is reminiscent of the behavior of dilute, isotropic solutions of PBLG. In such isotropic solutions, PBLG molecules aggregate in certain solvents, e.g., dioxane, benzene, ethylene dichloride.²⁹ Various modes of aggregation have been proposed: end-to-end, parallel, and antiparallel lateral associations.^{5,29} Although the nature of the intermolecular interactions responsible for aggregation is uncertain, there is general agreement that the addition to the solution of very small amounts of certain agents (dimethylformamide, formamide, dichloroacetic acid, and TFA) will break down the aggregates; the solution then acquires the properties of a dispersion of discrete PBLG helices.^{5,29} In the liquid crystal, aggregation of the PBLG would result in an intermittent three-dimensional gellike network with viscoelastic properties characteristic of melts of ordinary random-coil polymers. Destruction of the aggregated network would be accompanied by an increase in fluidity of the liquid crystal. The decrease in γ_1 at 1–2% TFA (Figure 3) and the apparent insensitivity of γ_1 at higher acid concentrations²² strongly suggest that PBLG aggregates in the liquid crystal in the manner observed in dilute solutions.

Studies of the bulk diamagnetic susceptibility of solid polypeptides have shown that 20% of the PBLG susceptibility can be attributed to the aromatic ring terminating the side chain.¹¹ The decrease in $\Delta\chi$ brought on by adding TFA to the PBLG liquid crystal (see Figure 3) is very likely due to a decrease in the contribution of the rather anisotropic ring to $\Delta\chi$ when side chain secondary structure is perturbed (see section B).

B. Microscopic Properties. Guha-Sridhar, Hines, and Samulski have previously suggested that measurements of the diamagnetic anisotropy could reveal aspects of the PBLG molecule's secondary structure.¹¹ Namely, information about the average orientation of the PBLG side chain could be obtained if $\Delta\chi$ can be separated into two contributions, $\Delta\chi^{\text{helix}}$ and $\Delta\chi^{\text{ring}}$. The former characterizes the anisotropy of the helical core of PBLG, the α -helical backbone plus part of the side chain, say, out to the α -carbon atom. The latter describes the anisotropy of the aromatic phenyl ring and benzyl CH_2 of the ester terminating the side chains of PBLG. The separation

can be carried out experimentally by subtracting $\Delta\chi^{\text{PGA}}$ found for a liquid crystal containing poly(L-glutamic acid) (PGA), a polypeptide which has no aromatic ring on the side chain, from $\Delta\chi^{\text{PBLG}}$. This amounts to equating $\Delta\chi^{\text{PGA}}$ to $\Delta\chi^{\text{helix}}$. According to eq 2, the subtraction

$$\Delta\chi^{\text{ring}} = \Delta\chi^{\text{PBLG}} - \Delta\chi^{\text{PGA}} \quad (4)$$

can be carried out when S is known (or has the same value) in both the PGA and PBLG liquid crystals. ($\Delta\chi$ is expressed in units of emu per mole of peptide residues.)

Recently, Murthy et al.³⁰ have determined S in the PBLG liquid crystal using x-ray diffraction. Their studies show that (a) S is insensitive to polypeptide concentration in the range 10–25% (wt/vol), (b) S does not vary with polypeptide axial ratio (molecular weight) in the range length/diameter = 70–140, and (c) for a given axial ratio and concentration of PBLG S decreases only marginally with increasing TFA concentration in the pretransition range 0–10% TFA. These results indicate that S is not strongly dependent on the detailed nature of the constituents and that a value of $S = 0.75$ is representative of the degree of order for all polypeptide liquid crystals in this class.

Since S changes very little in the pretransition range,³⁰ the rodlike shape of PBLG prevails throughout this range of TFA concentration; the observed change in $\Delta\chi^{\text{PBLG}}$ (Figure 3) implies a more subtle *intramolecular* structural change. Equation 4, when applied to the data in Figure 3 (assuming that S is the same in all polypeptide liquid crystals and that a previously determined value of $\Delta\chi^{\text{PGA}} = 2.58 \pm 0.3 \times 10^{-6}$ emu/mol¹¹), yields the behavior of $\Delta\chi^{\text{ring}}$ in the pretransition region (dashed line in Figure 3).

$\Delta\chi^{\text{ring}}$ can, with some assumptions, give information about the orientation of the phenyl ring relative to the helix axis, I . For a uniaxially symmetric distribution of side chains about the helix axis

$$\Delta\chi^{\text{ring}} = N_A(\sigma_l^{\text{ring}} - \sigma_t^{\text{ring}})S \quad (5)$$

where σ_l^{ring} and σ_t^{ring} are the average components of the ring diamagnetic susceptibility along the transverse to I , respectively:

$$\begin{aligned} \sigma_l^{\text{ring}} &= \sigma_a \overline{\cos^2 \alpha} + \sigma_b \overline{\cos^2 \beta} + \sigma_c \overline{\cos^2 \gamma} \\ \sigma_t^{\text{ring}} &= \frac{1}{2}\sigma_a \overline{\sin^2 \alpha} + \frac{1}{2}\sigma_b \overline{\sin^2 \beta} + \frac{1}{2}\sigma_c \overline{\sin^2 \gamma} \end{aligned} \quad (6)$$

σ_a , σ_b , and σ_c are the principal values of the ring susceptibility tensor along the Cartesian coordinate axes a , b and c (the c axis is normal to the ring plane, see Figure 6); α , β , and γ are the polar angles between I and the a , b , and c axes, respectively. The bar indicates an average over the distribution of side chain orientations. The ring orientation can be uniquely defined by specifying only two of the three orientation functions having the form $f_a = \frac{1}{2}(3 \cos^2 \alpha - 1)$, etc., which describe the average orientation of the a , b , and c axis. From eq 5 and 6,

$$\Delta\chi^{\text{ring}} = (\chi_a f_a + \chi_b f_b + \chi_c f_c)S \quad (7)$$

where $\chi_a = N_A \sigma_a$, etc., and $f_a + f_b + f_c = 0$.

It is useful to compare calculated values of $\Delta\chi^{\text{ring}}$ using previously reported static side chain conformations for PBLG with the experimentally determined value $\Delta\chi^{\text{ring}} = 4.2 \pm 0.8 \times 10^{-6}$ emu/mol (eq 4 and $\Delta\chi^{\text{PBLG}}$ without TFA). In Table I, values for α , β , and γ obtained from experimental and theoretical side chain conformations are listed. The former were derived from ir dichroism studies.³¹ The latter are computed low energy conformations which consider various contributions to the total conformational energy: bond rotational potentials, nonbonded van der Waals interactions, electrostatic interactions, and intermolecular perturbations.^{32,33} Values of $\Delta\chi^{\text{ring}}$ were calculated using eq 7 with the PBLG side chain benzyl fragment: $\chi_a = \chi_b = -39.9 \times 10^{-6}$ emu/mol and $\chi_c = -108.1 \times 10^{-6}$ emu/mol; $\frac{1}{3}(\chi_a + \chi_b + \chi_c)$ is the value found

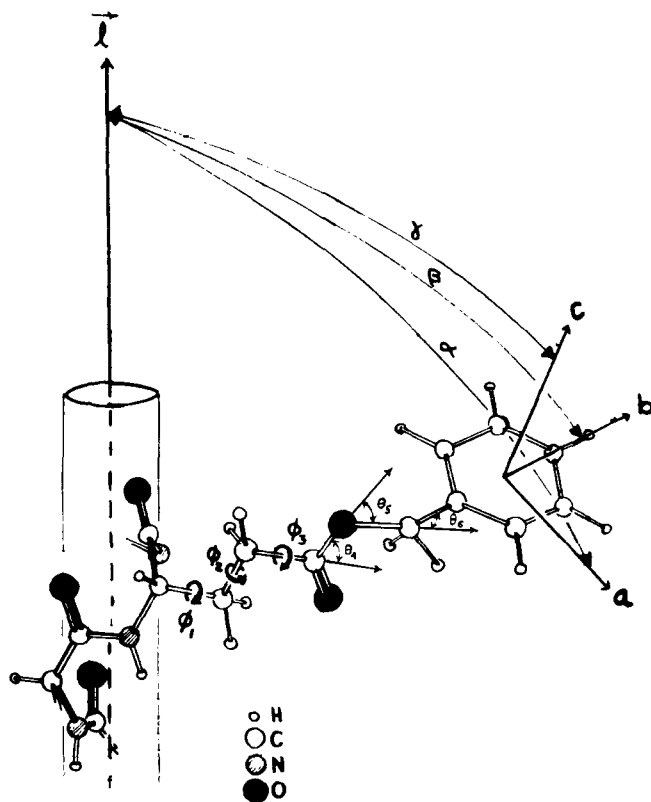


Figure 6. Schematic drawing of the PBLG side chain relative to the helix axis l ; a , b , and c axis form a Cartesian coordinate system with c normal to the ring plane (α , β , and γ are the polar angles); the ϕ_i are the dihedral angles describing configurations about side chain bonds 1–6; the θ_i are the supplements of the valence angles between bonds i and $i - 1$. ϵ_i (not shown) is the angle between l and bond i (eq 8 and 9).

for toluene (-64.54)³⁵ less one H atom (Pascal value -2.93).³⁶ The best agreement is obtained with Tsuboi's side chain conformation³¹ derived from ir studies of solid, oriented films of PBLG. However, the most striking aspect of this comparison with static conformations is the extreme sensitivity of the calculated $\Delta\chi^{\text{ring}}$ to small changes in α , β , and γ .

There is considerable experimental evidence both in solution and in the solid state that a good deal of internal motion occurs in the PBLG side chain. The line widths of the PBLG high resolution nuclear magnetic resonance (NMR) spectrum³⁷ and observed nuclear magnetic relaxation times³⁸ suggest rotational reorientation correlation times for the phenyl ring of the order of 10^{-10} s, only a factor of 10 longer than that of benzene itself. Dielectric and NMR studies of the solid state of PBLG indicate substantial side chain segmental motion.³³ The NMR second moment calculations for varying degrees of side chain internal motion yield best agreement with experiment (solid state; 20 °C) when free rotations of dihedral angles ϕ_6 and ϕ_5 (see Figure 6) are allowed, i.e., proton-proton nuclear dipolar interactions are effectively averaged by rotations about bonds 6 and 5 on a time scale of order 10^{-7} s.³³ Thus, it is very reasonable to assume that in the liquid crystal segmental motion within the PBLG side chain occurs and that such motion must be considered when calculating $\Delta\chi^{\text{ring}}$.

The experimental evidence cited above strongly suggests rapid rotation of the ring about bond 6 (rotation of dihedral angle ϕ_6). Since the potential barrier to rotation ϕ_6 has sixfold symmetry and is of the order of 0.5 kcal/mol,³² the motion would be symmetric, and the resulting expression for the averaging of the ring susceptibility derived from eq 7 is

$$\Delta\chi^{\text{ring}} = [\chi_b - \frac{1}{2}(\chi_a + \chi_c)]Sf_6 \quad (8)$$

where $f_6 = \frac{1}{2}(3 \cos^2 \epsilon_6 - 1)$ describes the average orientation

Table I. Calculated $\Delta\chi^{\text{ring}}$ for Specific Side Chain Conformations

| Model | Ref | α | β | γ | $\Delta\chi^{\text{ring } a}$ |
|---------------------------------------|-----|----------|---------|----------|-------------------------------|
| Tsuboi (ir dichroism) | 31 | 57 | 45 | 62 | +10.5 |
| Scheraga et al. ^b $R_1(+)$ | 32 | 90 | 28 | 62 | -8.4 |
| Scheraga et al. ^b $R_1(-)$ | 32 | 17 | 79 | 77 | +28.8 |
| Tanaka and Ishida (ir) | 33 | 65 | 48 | 69 | +35.6 |
| Tanaka and Ishida ^c A | 33 | 55 | 44 | 45 | -37.9 |
| Tanaka and Ishida ^d B | 33 | 51 | 62 | 65 | +28.1 |

^a Calculated with eq 7 using $S = 0.75$, $\chi_a = \chi_b = -39.9 \times 10^6$ emu/mol, and $\chi_c = -108.1 \times 10^{-6}$ emu/mol. ^b α , β , γ determined from model constructed according to calculated dihedral angles (see ref 32 for side chain nomenclature). ^c Lowest potential energy of side chain dihedral angles. ^d Side chain dihedral angles correspond to the Boltzmann distribution.

Table II. Calculated Orientation Functions of PBLG Side Chain Bonds

| Free rotation of dihedral angle ϕ_i | Calcd orientation function ^a | |
|---|---|-------|
| | Bond i | f_i |
| ϕ_6 | 6 | +0.16 |
| ϕ_6 and ϕ_5 | 5 | -0.48 |
| ϕ_6 , ϕ_5 , and ϕ_4 | 4 | +1.91 |
| ϕ_6 , ϕ_5 , ϕ_4 , and ϕ_3 | 3 | -15.3 |

^a Calculated with eq 8 and 9 using $\theta_6 = 70.5^\circ$, $\theta_5 = 66^\circ$, $\theta_4 = 60^\circ$, and $\Delta\chi^{\text{ring}} = 4.2 \times 10^{-6}$ emu/mol (no TFA).

of bond 6 relative to the helix axis, l ($\epsilon_6 = \beta$ and $f_6 \equiv f_b$ in eq 7). If, in addition to rotation of ϕ_6 , symmetric rotation is allowed about successive dihedral angles in the side chain (ϕ_5, \dots, ϕ_i), $\Delta\chi^{\text{ring}}$ is given by

$$\Delta\chi^{\text{ring}} = [\chi_b - \frac{1}{2}(\chi_a + \chi_c)]Sf_i \prod_{j=i}^5 P_2(\cos \theta_{j+1}), i \leq 5 \quad (9)$$

The factors $P_2(\cos \theta_{j+1}) = \frac{1}{2}(3 \cos^2 \theta_{j+1} - 1)$ account for the averaging caused by rotation of ϕ_j ; θ_{j+1} is the supplement of the valence angle between bonds j and $j + 1$ (see Figure 6). $f_i = \frac{1}{2}(3 \cos^2 \epsilon_i - 1)$ describes the average orientation of bond i relative to the helix axis. For perfect alignment, $f_i = 1$ if bond i is parallel to l and $f_i = -0.5$ if bond i is perpendicular to l . $f_i = 0$ for a random distribution of bond orientations and the highly improbable situation that bond i is fixed at the "magic" angle ($55^\circ 44'$) relative to l .

Equations 8 and 9 provide a convenient way of examining the effects of proposed side chain motions. The orientation functions can be calculated by solving eq 8 for f_6 and eq 9 for f_i , $i = 1-5$, using side chain valence angles θ_i , the values for $\chi_{a,b,c}$ above, $S = 0.75$, and the experimentally determined $\Delta\chi^{\text{ring}}$. Table II lists the calculated values of f_i related to varying degrees of rotational freedom, i.e., rotations of the ϕ_i 's are introduced by beginning with the periphery of the side chain (ϕ_6) and progressively allowing rotational freedom about successive bonds of the side chain inward to the helix. We find unreasonable values of f_i if, in addition to free rotation of ϕ_6 and ϕ_5 , rotation is allowed about bonds 4, 3, 2, and 1 (the f_i must lie in the range +1.0 to -0.5). That is, f_i for $i < 5$ and concomitant motional averaging is not consistent with the measured diamagnetic anisotropy. For rotation of ϕ_6 and ϕ_5 we find an extreme value $f_5 \approx -0.5$ implying that bond 5 would be constrained to an orientation essentially perpendicular to the helix axis.

Either orientation function, f_6 or f_5 , provides a parameter for monitoring the change in side chain reorientational mobility in the pretransition region. Figure 7 shows f_6 and f_5 as a function of TFA concentration in the liquid crystal calculated

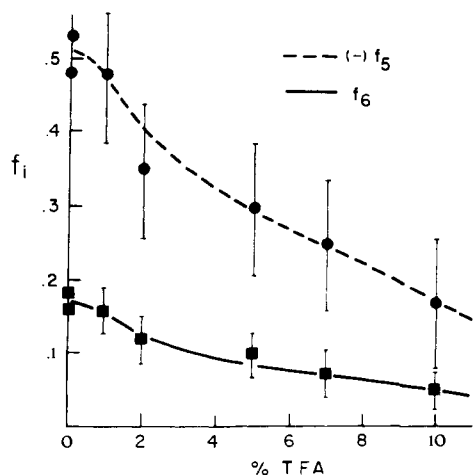


Figure 7. The orientation functions f_6 (■, —) and f_5 (●, - -) calculated with eq 8 and 9 as a function of % TFA (vol) in PBLG-dioxane:TFA liquid crystals. The average orientation of bonds 6 and 5 relative to the helix axis decreases as acid is added to the liquid crystal.

from eq 8 and 9 and the data in Figure 3. The average orientation of bonds 6 and 5 decreases with increasing TFA approaching that for an isotropic distribution, $f_6 = f_5 = 0$. At 7 and 10% TFA, f_4 (free rotation about ϕ_6 , ϕ_5 , and ϕ_4) assumes reasonable values, +1.0 and +0.7, respectively. This suggests that at high concentrations of TFA, the averaging of the ring susceptibility tensor caused by free rotation of ϕ_6 , ϕ_5 , and ϕ_4 is consistent with measured anisotropies.

V. Conclusions

In the last few years NMR studies of model compounds³⁹ and helix-coil transitions in nonprotonating solvents⁴⁰ have produced new insights into the mechanism of solvent-induced denaturation of PBLG. The original mechanism proposed for the acid-induced helix-coil transition, protonation of the amide linkage in the PBLG backbone, has given way to a putatively less severe interaction of TFA with PBLG. Ir studies indicate protonation of, or hydrogen-bond formation with, the PBLG side chain ester group.³ In general, there has been increasing evidence that the polypeptide side chain, especially that with an aromatic group, is integrally related to the helix conformation and stability.⁴¹ This evidence plus that obtained from investigations of dynamic aspects of the helix-coil transition (nuclear Overhauser effect,⁴² high resolution NMR,^{6,22} nuclear relaxation^{4,38}) and the magnetic susceptibility data reported here clearly demonstrate that prior to the helix-coil transition, there is a change in mobility of the PBLG side chains. Previous investigations of pretransition phenomena in dilute solution strongly implied that the helix backbone remains rigid in this range of TFA concentration.³ More recent studies in liquid crystals suggest an increase in helix flexibility, i.e., the rodlike shape of PBLG is preserved while breaks in the helix rapidly propagate along the chain.²² Our susceptibility data imply that the increased molecular mobility is localized primarily within the side chain secondary structure.

Although there is overwhelming evidence implicating side chain segmental motion in the pretransition range, a choice between orientation functions f_5 and f_6 to quantify this motion based on the magnetic data alone is quite arbitrary. In the absence of TFA, the selection of $f_6 = +0.16$ to describe the average orientation amounts to lumping together all possible types of segmental motion (rotations of dihedral angles ϕ_1 through ϕ_5 , wagging of the end of the side chain due to conformation changes, etc.) to produce a more general kind of order parameter. On the other hand, a choice of $f_5 \approx -0.5$ allows only those configurations of the preceding side chain segments (bonds 1–4) which result in an orientation of bond

5 normal to the helix axis; i.e., it allows only restricted and correlated side chain motion. Also, for this choice, we must consider the reasonableness of the associated averaging motions: rotation of the ring about bond 6 and, rotation about bond 5 (movement of the ring about the surface of a cone of arc $2\theta_6$). Unhindered rotation about bond 6 is plausible but free rotation for dihedral angle ϕ_5 seems somewhat less so, especially in view of steric constraints imposed by neighboring side chains.

Either f_5 or f_6 suffices as an indicator of increased side chain mobility as TFA is added to the liquid crystal and Figure 7 presents strong evidence for disruption of a side chain secondary structure of PBLG by TFA at low acid concentrations prior to the TFA-induced helix-coil transition. These experimental measurements do not give new information about the mode of association of TFA with the PBLG side chain. A more detailed analysis of the dynamics of side chain segmental motion in the pretransition range can, however, be obtained from NMR investigations in the liquid crystal phases.⁴³

This work demonstrates that investigations of conformational aspects of polypeptides in the liquid crystal phase are feasible, and that the macroscopic properties of this aggregated state exhibit behavior paralleling that reported in dilute solution studies of pretransition phenomena. In addition, the pitch of the cholesteric texture and the anisotropic magnetic characteristics of oriented polypeptide liquid crystals are found to provide new points of departure from which to probe subtle aspects of polypeptide molecular conformation.

Acknowledgment. We are very grateful to Dr. H. T. Edzes for many helpful discussions during the preparation of this manuscript. Also, we wish to thank Ms. M. Langell for her technical assistance and Ms. M. C. Shumate for her efforts to pare the verbage.

References and Notes

- (1) This investigation was supported in part by a NIH research grant (PHS Grant AM 17497-02) from the National Institute of Arthritis, Metabolism and Digestive Diseases and The University of Connecticut Research Foundation.
- (2) (a) University of Louisville; (b) University of Connecticut.
- (3) (a) D. Poland and H. A. Scheraga, "Theory of Helix-Coil Transitions in Biopolymers", Academic Press, New York, N.Y., 1970; (b) G. D. Fasman, Ed., "Poly- γ -amino Acids", Vol. 1, Marcel Dekker, New York, N.Y., 1967; (c) J. B. Millstein and E. Charney, *Biopolymers*, **9**, 991 (1970).
- (4) E. T. Samulski, M. Chien, and C. G. Wade, *J. Polym. Sci., Polym. Symp.*, **No. 46**, 335 (1974).
- (5) A. K. Gupta, C. Dufour, and E. Marchal, *Biopolymers*, **13**, 1293 (1974).
- (6) D. I. Marlborough, K. G. Orrell, and H. N. Rydon, *Chem. Commun.*, 518 (1965).
- (7) E. M. Bradbury, C. Crane-Robinson, and H. W. E. Rattle, *Polymer*, **11**, 277 (1970).
- (8) C. Robinson, *Tetrahedron*, **13**, 219 (1961).
- (9) A photomicrograph of these unusual patterns of retardation lines is shown on p 908 of "Physical Chemistry", 3rd ed, W. J. Moore, Prentice-Hall, Englewood Cliffs, N.J.
- (10) S. Sobajima, *J. Phys. Soc. Jpn.*, **23**, 1070 (1967); M. Panar and W. D. Phillips, *J. Am. Chem. Soc.*, **90**, 3880 (1968); E. T. Samulski and A. V. Tobolsky, *Macromolecules*, **1**, 555 (1968).
- (11) C. Guha-Sridhar, W. A. Hines, and E. T. Samulski, *J. Chem. Phys.*, **61**, 947 (1974).
- (12) E. T. Samulski, unpublished results.
- (13) R. B. Meyer, *Appl. Phys. Lett.*, **14**, 208 (1968).
- (14) P. G. de Gennes, *Solid State Commun.*, **6**, 163 (1968).
- (15) P. D. de Gennes, *Mol. Cryst. Liq. Cryst.*, **7**, 325 (1969).
- (16) R. W. Duke and D. B. Du Pré, *J. Chem. Phys.*, **60**, 2757 (1974).
- (17) D. B. Du Pré and R. W. Duke, *J. Chem. Phys.*, **63**, 143 (1975).
- (18) P. G. de Gennes, "The Physics of Liquid Crystals," Clarendon Press, Oxford, 1974, Chapter II.
- (19) C. Guha-Sridhar, W. A. Hines, and E. T. Samulski, *J. Phys. (Paris), Colloq.*, **36**, 270 (1975).
- (20) E. T. Samulski and H. J. C. Berendsen, *J. Chem. Phys.*, **56**, 3921 (1972).
- (21) J. Pelletier and E. T. Samulski, unpublished results.
- (22) P. Laszlo, A. Paris, and E. Marchal, *J. Phys. Chem.*, **77**, 2925 (1973).
- (23) R. W. Filas, L. E. Hajdo, and A. C. Eringen, *J. Chem. Phys.*, **61**, 3037 (1974).
- (24) The form optical rotation referred to here should not be confused with the behavior of a chiral or optically active molecule in the vicinity of an absorption band. The latter optical rotation occurs in isotropic dilute solutions which contain optically active molecules and has its origin in the selective absorption of one circularly polarized component of the light. The form optical rotation which we are discussing is caused by the *supramolecular arrangement* of the PBLG rods in the cholesteric structure and originates in the selective reflection of circularly polarized light by this structure.

- (25) See footnote 15 in ref 8.
 (26) W. J. A. Goossens, *Mol. Cryst. Liq. Cryst.*, **12**, 237 (1971).
 (27) Reference 3b, Chapter IX.
 (28) E. T. Samulski, Ph.D. Dissertation, Department of Chemistry, Princeton University, 1969.
 (29) J. C. Powers and W. L. Peticolas, *Biopolymers*, **9**, 195 (1970).
 (30) S. Murthy, J. R. Knox, and E. T. Samulski, in preparation.
 (31) M. Tsuboi, *J. Polym. Sci.*, **59**, 139 (1962).
 (32) J. F. Yan, G. Vanderkooi, and H. A. Scheraga, *J. Chem. Phys.*, **49**, 2713 (1968).
 (33) A. Tanaka and Y. Ishida, *J. Polym. Sci., Polym. Phys. Ed.*, **11**, 1117 (1973).
 (34) J. Hoarau, N. Lumbruso, and A. Pacault, *C. R. Hebd. Seances Acad. Sci.*, **242**, 1702 (1956).
 (35) C. M. French, *Trans. Faraday Soc.*, **50**, 1320 (1954).
 (36) P. W. Selwood, "Magnetochemistry", Interscience, New York, N.Y., 1956, Chapter VI.
 (37) E. M. Bradbury, B. G. Carpenter, C. Crane-Robinson, and H. Goldman, *Nature* (London), **225**, 64 (1970).
 (38) M. Chien, E. T. Samulski, and C. G. Wade, *Macromolecules*, **6**, 638 (1973).
 (39) F. A. Bovey, "High Resolution NMR of Macromolecules", Academic Press, New York, N.Y., 1972, Chapter XIII.
 (40) E. M. Bradbury, C. Crane-Robinson, L. Paolillo, and P. Temussi, *Polymer*, **14**, 303 (1973).
 (41) M. Goodman, G. W. Davies, and E. Benedetti, *Acc. Chem. Res.*, **1**, 275 (1968).
 (42) A. A. Bothner-By and Gassend, *Ann. N.Y. Acad. Sci.*, **222**, 668 (1973).
 (43) Preliminary investigations of hyperfine interactions in anisotropic PBLG liquid crystals by ^{13}C NMR indicate that segmental motions in the side chain are rapid (correlation times for reorientation $< 10^{-7}$ s). H. T. Edzes and E. T. Samulski, work in progress.
 (44) NOTE ADDED IN PROOF. Recent calculations of van der Waals-Lifshitz forces between chiral rods suspended in a dielectric medium indicate that $P_0 \rightarrow \infty$ for certain values of the dielectric constant of the medium (E. T. Samulski, manuscript in preparation).

Thermodynamics of Molecular Association. 9. An NMR Study of Hydrogen Bonding of CHCl_3 and CHBr_3 to Di-*n*-octyl Ether, Di-*n*-octyl Thioether, and Di-*n*-octylmethylamine

D. E. Martire,* J. P. Sheridan, J. W. King, and S. E. O'Donnell

Contribution from the Department of Chemistry, Georgetown University, Washington, D.C. 20057. Received August 28, 1975

Abstract: Nuclear magnetic resonance studies in the temperature range 10 to 40 °C are reported for the hydrogen bonding between the electron acceptors and donors of the title, all in cyclohexane solution. Data on the variation of the chemical shifts of the haloform C-H proton as a function of donor concentration are treated by the Foster-Fyfe procedure which permits direct determination of the equilibrium constants, K , for 1:1 hydrogen-bonded complex formation. The results are discussed in terms of Deranleau's criteria for reliability of the results and proof of fit of the proposed model. Enthalpies and entropies of hydrogen bonding are determined from the variation of $\ln K$ with temperature. The thermodynamic constants so obtained and thermodynamic data previously determined by gas-liquid chromatography are used to evaluate thermodynamic parameters related to halogen/*n*-donor interaction. Consistent with other evidence and a polarization experiment reported here, the latter interactions are taken to involve negligible complex formation. The enthalpies of halogen/*n*-donor interaction are found to follow the trends $\text{CHBr}_3 > \text{CHCl}_3$ and $\text{N} > \text{S} > \text{O}$. The enthalpies of hydrogen bonding, which follow the trends $\text{CHCl}_3 > \text{CHBr}_3$ and $\text{N} > \text{O} > \text{S}$, are analyzed in terms of the double-scale equation of Drago.

In parts 2¹ and 4² of this series we presented thermodynamic data (termed equilibrium constants, enthalpies, and entropies of "complex formation") from gas-liquid chromatography (GLC) for the interaction of CHCl_3 , CHBr_3 , and other haloalkane acceptors with four *n*-electron donors: di-*n*-octyl ether (DOE), di-*n*-octyl thioether (DOTE), di-*n*-octylmethylamine (DOMA), and tri-*n*-hexylamine (THA). Analysis of the results obtained strongly indicated the presence of two types of interactions within these systems: (1) hydrogen bonding of the C-H hydrogen of the haloalkane to the *n*-donor atom, (2) charge transfer ($n \rightarrow \sigma^*$ type)-and/or electrostatic interaction between the *n*-donor and halogen atoms.

It has been pointed out¹ that thermodynamic measurements *alone* cannot serve to establish the existence of molecular complexes. Moreover, it has been shown recently³ that the generally accepted GLC methods for obtaining "association constants" yield, in fact, a quantity which is the sum of the equilibrium constant (K_1) for all 1:1 complex formation and a term (α) which reflects any noncomplexing acceptor-donor interactions present in the system, i.e., " K_{GLC} " = $K_1 + \alpha$. Hence, given the overwhelming spectroscopic evidence¹ that haloalkanes (such as CHCl_3 and CHBr_3) do indeed form hydrogen-bonded complexes with *n*-donors, we were left with two *simple* interpretations of the " K_{GLC} " data: (1) " K_{GLC} " = ($K + K'$), where K and K' are the 1:1 association constants for

hydrogen-bonded and halogen-bonded complex formation, respectively, or (2) " K_{GLC} " = ($K + \alpha$), where α is a measure of noncomplexing halogen/*n*-donor interaction or contact pairing.^{3,4} For lack of any conclusive evidence, one way or the other (see below), we arbitrarily chose the former description. Nevertheless, the qualitative discussion of the " K_{GLC} " and concomitant enthalpy (which reflects a weighted average of all pairwise interactions) presented in parts 2 and 4 turns out to be equally valid for either description.

The nature of halogen/*n*-donor interactions in these systems, however, is an unsettled matter.^{1,2} Charge-transfer bands (attributed to $n \rightarrow \sigma^*$ transitions) have been found in the ultraviolet region for several tetrahalomethane/amine systems,^{5,6} but the reliability of the derived K values ($K < 0.1$ l. mol⁻¹ for FCCl_3 , ClCCl_3 , and BrCCl_3 with triethylamine,⁵ and $K \approx 0.03$ l. mol⁻¹ for CCl_4 /*n*-butylamine⁶) is open to question.⁶⁻⁸ Values this small indicate little or no complex formation and can hardly account for the " K_{GLC} " values and trends observed in parts 2 and 4. Also, no charge-transfer bands have been reported¹ or found in our laboratory for mixtures of CBr_4 or CCl_4 and ether or thioether donors. Hence, while much thermodynamic, spectroscopic, and structural evidence¹ exists for strong halogen/*n*-donor interactions, it is not clear whether substantial complex formation is involved, or whether charge-transfer interactions play an important role. With re-